LWT - Food Science and Technology 222 (2025) 117641

Contents lists available at ScienceDirect

LWT

journal homepage: www.elsevier.com/locate/lwt

Peptide from tempeh-like fermented *Chenopodium formosanum* counters senescence while enhancing antioxidant ability in non-replicative aging

Chen-Che Hsieh [a,1], Hui-Wen Lin [b,c,1], Hsiao-Chu Huang [d], Darin Khumsupan [e], Szu-Chuan Shen [f], Shin-Ping Lin [g,h,i], Chang-Wei Hsieh [j,k], Tsung-Yu Tsai [l], Sirima Suvarnakuta Jantama [m], Hsing-Chun Kuo [n,o,p,q,*], Kuan-Chen Cheng [d,e,l,r,s,**]

[a] *Department of Seafood Science, National Kaohsiung University of Science and Technology, No. 142, Haijhuan Rd., Nanzih District, Kaohsiung, 81157, Taiwan R.O.C*
[b] *Institute of Medicine, Chun Shan Medical University, Taichung, Taiwan R.O.C*
[c] *Department of Medical Research, Chung Shan Medical University Hospital, Taichung, Taiwan R.O.C*
[d] *Institute of Food Science and Technology, National Taiwan University, No. 1, Sec. 4, Roosevelt Rd., Taipei, Taiwan R.O.C*
[e] *Institute of Biotechnology, National Taiwan University, No. 1, Sec. 4, Roosevelt Rd., Taipei, Taiwan R.O.C*
[f] *Undergraduate and Graduate Programs of Nutrition Science, School of Life Science, National Taiwan Normal University, Taipei, Taiwan R.O.C*
[g] *School of Food Safety, Taipei Medical University, 250 Wu-Hsing Street, Taipei 11042, Taiwan R.O.C*
[h] *Ph.D. Program in Drug Discovery and Development Industry, College of Pharmacy, Taipei Medical University, 250 Wu-Hsing Street, Taipei 11031, Taiwan R.O.C*
[i] *Research Center of Biomedical Device, Taipei Medical University, 250 Wu-Hsing Street, Taipei 11031, Taiwan R.O.C*
[j] *Department of Food Science and Biotechnology, National Chung Hsing University, 145 Xingda Rd, South Dist, Taichung, 40227, Taiwan R.O.C*
[k] *Department of Food Science, National Ilan University, No. 1, Sec. 1, Shennong Rd., Yilan City, Yilan County, 260007, Taiwan R.O.C*
[l] *Department of Food Science, Fu Jen Catholic University, No. 510, Zhongzheng Rd., Xinzhuang Dist., New Taipei City, 242062, Taiwan R.O.C*
[m] *Faculty of Pharmaceutical Sciences, Ubon Ratchathani University, Warinchamrap, Ubon Ratchathani, 34190, Thailand*
[n] *Department of Nursing, Division of Basic Medical Sciences, Chang Gung University of Science and Technology, Chiayi, Taiwan R.O.C*
[o] *Research Fellow, Chang Gung Memorial Hospital, Chiayi, Taiwan R.O.C*
[p] *Chronic Diseases and Health Promotion Research Center, Chang Gung University of Science and Technology, Chiayi, Taiwan R.O.C*
[q] *Research Center for Food and Cosmetic Safety, College of Human Ecology, Chang Gung University of Science and Technology, Taoyuan, Taiwan R.O.C*
[r] *Department of Optometry, Asia University, 500, Lioufeng Rd., Wufeng, Taichung, Taiwan R.O.C*
[s] *Department of Medical Research, China Medical University Hospital, China Medical University, 91, Hsueh-Shih Road, Taichung, Taiwan R.O.C*

ARTICLE INFO

Keywords:
Chenopodium formosanum
Glycine-rich peptides
Non-replicative aging
Nrf2 pathway
Oxidative stress

ABSTRACT

The study assesses the protective effects of glycine-rich peptide (GRP) from tempeh-like fermented *Chenopodium formosanum* against non-replicative aging. By pretreating Hs68 cells with GRP and irradiating them with UVA, a reduction in oxidative stress was observed which positively contributed to cell survival rate. Moreover, transcriptomic analysis demonstrated that pretreatment with GRP prevents the downregulation of oxidative stress responses and an upregulated expression of cell cycle. Additionally, GRP was found to increase the expression of Nrf2 pathway while decreasing the expressions of *p53* and *p21*. These findings were further investigated in *Caenorhabditis elegans*, where GRP treatment could extend lifespans and improve resistance to oxidative stress. Finally, molecular docking studies indicated GRP binds to the KEAP-BTB inhibitory site inhibitory site, potentially inhibiting activity of single O-linked β-N-acetylglucosamine transferase which facilitates activation of Nrf2

Abbreviations: ACE, angiotensin-converting enzyme; ARE, antioxidant response element; CCK-8, cell counting kit-8; BP, biological process; ChIP, chromatin immunoprecipitation; c-Fos, fos proto-oncogene; c-Jun, jun proto-oncogene; DEGs, differential expression genes; DPP4, dipeptidyl peptidase-4; DMSO, dimethyl sulfoxide; FCS, fermented *Chenopodium formosanum* sprouts; FudR, floxuridine; gcs, glutamylcysteine synthetase; GO, gene ontology; GRP, glycine-rich peptide; GSR, glutathione reductase; gst, glutathione S-transferase; HO-1, heme oxygenase-1; IIS pathway, insulin/insulin-like signaling pathway; Keap1-BTB, kelch-like ech-associated protein 1- broad complex, tramtrack, and bric-a-brac; *Mus musculus*, Mouse reference genome; NAC, N-acetylcysteine; NF-kB, Nuclear factor kappa B; NGM agar, nematode growth medium; Nrf2, nuclear factor, erythroid 2; NQO1, NAD(P)H: quinone oxidoreductase 1; OGT, single O-linked β-N-acetylglucosamine transferase; *p53*, cellular tumor antigen; *p21*, cyclin-dependent kinase inhibitor 1; ROS, reactive oxygen species; *Skn-1*, transcription factor skinhead-1; SA-β-Gal, senescence-associated β-galactosidase; SOD, superoxide dismutase 1; UV, ultraviolet.

* Corresponding author. Department of Nursing, Division of Basic Medical Sciences, Chang Gung University of Science and Technology, Chiayi, Taiwan, ROC.
** Corresponding author. Institute of Food Science and Technology, National Taiwan University, No. 1, Sec. 4, Roosevelt Rd., Taipei, Taiwan, ROC.
E-mail address: kccheng@ntu.edu.tw (K.-C. Cheng).

[1] Dr. Chen-Che Hsieh and Dr. Hui-Wen Lin did the same contribution on this research.

https://doi.org/10.1016/j.lwt.2025.117641
Received 23 January 2025; Received in revised form 7 March 2025; Accepted 11 March 2025

pathway. These results highlight the capability of GRP as a protective agent against oxidative stress and non-replicative aging.

1. Introduction

Chenopodium formosanum is a pseudo-cereal native to Taiwan which is commonly known as Taiwanese quinoa (Huang and Chien, 2020). *C. formosanum* is rich in nutrients and antioxidants, which can potentially serve as an excellent precursor of bioactive peptides (Kuo et al., 2021). As a result, the fermentation of *C. formosanum* can further amplify these bioactive ingredients. Hsieh, Yu, Cheng, et al. (2023) used *R. oligosporus,* which possesses rich proteolytic enzymes, to ferment *C. formosanum* and discovered seven new glycine-rich peptides from the hydrolysate which can act as antioxidants, reducing intracellular oxidative stress (Hsieh, Yu, Cheng, et al., 2023), One glycine-rich peptide (GGGGGKP) obtained from fermented *C. formosanum* can reduce exogenous oxidative stress by regulating the phosphorylation of NF-κB, inducing anti-inflammatory and ROS suppression effects. The preparation method for this glycine-rich peptide involved initially obtaining a low-molecular-weight protein fraction using MWCO. This was followed by desalting and gel filtration through FPLC, using Sephadex G-25 superfine and Superdex 30 Increase SEC column to isolate a single peptide. Subsequently, LC-ESI-Q-TOF-MS/MS analysis was performed, and the peptide sequence composition was confirmed by matching against a database (Hsieh, Yu, Cheng, et al., 2023).

Furthermore, other glycine-rich peptides (GGLGDVLGGLP and GEGW) derived from food or plants such as *C. quinoa* and *Acheta domesticus*, served as promising protectants against free radicals and oxidative stress due to their unique sequence compositions (Mirzaei et al., 2018; Ren et al., 2022; Vilcacundo et al., 2017). This phenomenon is due to *R. oligosporus* utilizing its endogenous enzymes (amylase, β-glucosidase, and proteinase) to cleave covalently bound phenolic compounds from cell walls of the plant substrates, metabolizing them into small hydrophobic peptides and phenolic compounds. Moreover, it was found that these bioactive peptides do not cause bioaccumulation (Guo et al., 2023; Hsieh et al., 2023). Therefore, the tempeh-like fermented *C. formosanum* may potentially possess multiple antioxidants, anti-ACE, and anti-DPP4 agents (Hsieh, Yu, Kuo, et al., 2023)·

Many studies have shown that substances extracted from natural fruits and herbs possess antioxidant activity and can modulate relevant signaling pathways to achieve bioactive effects. For instance, myricitrin from Chinese bayberry has been found to prevent peroxynitrite-mediated glutathione depletion in astrocytes. Flavonoids in tartary buckwheat have demonstrated both antioxidant and antidiabetic effects. Additionally, lemon verbena has been shown to exert antioxidative properties that delay damage under glucotoxic conditions in adipocytes. Therefore, it is feasible to use bioactive substances from natural fruits and herbs to regulate diseases induced by oxidative stress (Bao et al., 2016; Chen et al., 2013; Olivares-Vicente et al., 2024).

Recent studies have demonstrated that microbial strains such as *Lactobacillus*, and *Rhizopus* can generate bioactive peptides with antioxidant and anti-aging properties. Hydrolysis using lactic acid bacteria (LAB) has been shown to produce bioactive peptides with improved antioxidant activity and reduced cellular protein production, presenting a promising strategy for developing functional foods with enhanced nutritional benefits (Lee et al., 2023). Bioactive peptides from fermented *C. formosanum* sprouts have shown potential as antioxidant agent (Hsieh, Yu, Cheng, et al., 2023). *C. formosanum* protein releases bioactive peptides during germination, fermentation, and digestion. Enzymatic hydrolysis using microbial fermentation and bioconversion is the primary method for preparing these peptides. The hydrolysate is assessed for biological activities, such as angiotensin I converting enzyme and antioxidant effects (Hsieh, Yu, Kuo, et al., 2023). Atmospheric radiation, a main factor in photoaging, produces ROS, damaging proteins, lipids, nucleic acids, and cell membranes, leading to reduced cellular integrity and mitochondrial dysfunction. Bioactive peptides may use their antioxidant properties to mitigate oxidative stress caused by photoaging (Lu et al., 2023).

Non-replicative aging stems from the free radical theory which posits that excessive free radicals produced during mitochondrial metabolic processes, such as cellular respiration, play a significant role in aging (Nandita et al., 2020). This concept has been validated by numerous *in vitro* and in vivo models that simulate the damages caused by free radicals. For instance, UV radiation-induced ROS in skin cells leads to photoaging (Fu et al., 2014; Huang & Chien, 2020), and the resulting ROS stimulates cellular pathways which ultimately triggers the release of inflammatory cytokines (Salminen et al., 2022). In addition, the production of ROS can be influenced by the insulin/insulin-like signaling (IIS) pathway. One study examined IIS pathway (SKN-1/NRF2) in nematodes and discovered that it could serve as a method to predict life span (Xiong et al., 2021). Consequently, examining gene expression associated with IIS pathways in an animal model may be a practical tool to verify the biological activity of substances extracted from food (Ye et al., 2021).

This study investigates the anti-aging effects of glycine-rich peptide (GRP) from fermented *C. formosanum* sprout. Employing Hs68 cells and *Caenorhabditis elegans* as the models, GRP's abilities to enhance cell viability, reduce oxidative stress, and its impact on aging-related enzymes and genes, mainly through the Nrf2 pathway, are investigated. This study seeks to establish its unique advantages in mitigating oxidative stress and extending lifespan. By addressing the gap in knowledge regarding the role of GRPs in non-replicative aging, this study contributes to the growing field of functional food research and the development of dietary interventions for age-related oxidative stress management.

2. Materials and methods

2.1. Materials

C. formosanum grains were purchased from Quinoa Green Biotech Co., Ltd (Taichung, Taiwan). *Rhizopus microsporus* var. *oligosporus* BCRC 31996 and human foreskin fibroblast (Hs68) cell line were obtained from Bioresource Collection and Research Center (BCRC) (Hsinchu, Taiwan). *Caenorhabditis elegans* and *Escherichia coli* OP50 were obtained from the National Core Facility for Biopharmaceuticals (Taipei, Taiwan). Medium ingredients such as peptone, yeast extract, potato dextrose broth, lysogeny broth, and agar were purchased from BioShop Canada Inc. (Ontario, Canada). EDTA solution, trypsin, and antibiotics (penicillin/streptomycin) were purchased from GE Healthcare Life Science (Logan, Utah, U.S.A). Vivaspin 15R and Vivaspin Turbo 15 were obtained from Sartorius Stedim Biotech GmbH (Goettingen, Germany). Cell culture media (Dulbecco's Modified Eagle Medium, or DMEM, supplemented with high glucose, phenol red, and L-glutamine) and fetal bovine serum were retrieved from GE Healthcare Life Science. Senescence β-Galactosidase Staining Kit (Abbkine, Inc., Wuhan, China) and Radio-Immunoprecipitation Assay (RIPA) Buffer (10X) were obtained from Cell Signaling Technology (Beverly, MA, U.S.A). CCK-8 was purchased from Cyrus Bioscience (Neihu, Taiwan). Nrf2 antibody (GTX103322) was purchased from GeneTex (Hsinchu, Taiwan). All chemicals used in this study were of analytical grade and purchased from Merck (Burlington, MA, U.S.A).

2.2. Preparation of FCS

C. formosanum sprouts, weighing 1.5 kg (wet condition, the moisture content was 63.25 ± 4.15 g/100 g), were subjected to sterilization in a bioreactor (FS-V-SA05P, Major Science, Taoyuan, Taiwan). The sterilization process was carried out for 20 min at 121 °C. Subsequently, 75 mL of *R. oligosporus* spores, with the concentration of 10^6 spores/mL (constituting 5 mL/100 g of the total), were inoculated onto the sterilized sprouts. The methodology employed for the solid-state fermentation process was referred from previous research (Hsieh, Yu, Kuo, et al., 2023), which involved maintaining the temperature of 35 °C, aeration volume of 0.4 vvm (air volume/culture volume/min), and rotation speed at 5 rpm. The fermentation duration was set to four days. After the fermentation, all the fermented products were collected and stored at −20 °C.

2.3. Isolation of GRP from FCS proteins

The glycine-rich peptide was prepared as descripted in previous research (Hsieh, Yu, Cheng, et al., 2023). Briefly, the lyophilized FCS was ground into powder, sieved through a 30-mesh screen, and stored at −20 °C. The FCS was degreased by submerging it in n-hexane (1:3 w/v) at 37 °C for 2 h. After drying the mixture with a rotary vacuum evaporator, the degreased FCS sample was mixed with phosphate-buffered saline (1:10 w/v) until homogenized. The homogenized sample was centrifuged at 15,000×*g* for 30 min at 4 °C, yielding a supernatant. This supernatant was heated to 70 °C to inactivate enzymes. Following a referenced protein extraction method, ammonium sulfate was added to the FCS supernatant to reach 90 % saturation, inducing salting-out. The resultant mixture was again centrifuged under similar conditions to collect protein precipitate. Afterward, GRP from FCS was purified using Superdex 30 Increase SEC column with fast protein liquid chromatography (ÄKTA purifier UPC 10, GE Healthcare Life Science, Utah, USA). The flow rate was set to 0.5 mL/min. Standards including Gly-Tyr, Leu enkephalin, Met enkephalin, and Val-Tyr-Val were used in the detection of glycine-rich peptide. The sequence of glycine-rich peptide is Gly- Gly-Gly- Gly- Gly-Lys-Pro, which was identified by BIOTOOLS Biotechnology Co., Ltd. (Taipei, Taiwan) (Hsieh, Yu, Kuo, et al., 2023).

2.4. Cell culture and UVA irradiation

The cells underwent pretreatment with 50 and 100 μg/mL GRP, which were diluted in serum-free DMEM, for a duration of 24 h. Subsequently, the cells were washed with 100 μL of PBS, followed by 100 μL of phenol red-free DMEM. For UV-A irradiation, the cells in a 96-well plate were positioned directly under the UVP crosslinkers (365 nm, Chingtek Instrument Co., Ltd., New Taipei, Taiwan). The Hs68 cells were positioned 10 cm away from an UVP crosslinkers and were exposed to UVA radiation at a dose of 15 J/cm^2 ($\lambda_{\max}$, 365 nm) for approximately 75 min (Hsiao et al., 2023; Lu et al., 2023). The irradiation dose was calculated based on Equation (2.1). 1 mmol/L NAC was used as positive control.

$$\text{Dosage}\ (\text{J}/\text{cm}^2) = \text{Intensity}\ (\text{mW}/\text{cm}^2) * \text{time} \qquad (\text{Equation 2.1})$$

2.5. Cell viability

In the cell viability assessment, the Cell Counting Kit-8 (CCK-8, Dojindo Molecular Technologies, Inc., Rockville, MD, USA) was employed and the procedure was based on the manufacturer's instructions (Hsiao et al., 2023).

2.6. ROS production

In the study, 5×10^5 cells were seeded in each well of a 96-well plate. These cells were then pretreated with the GRP at a concentration of 50 and 100 μg/mL for 24 h. After GRP was removed, the cells were subjected to UVA exposure at a dose of 15 J/cm^2. Subsequently, H_2DCFDA was added, and the cells were cultured for an additional 30 min. Imaging was performed using a fluorescent microscope. The relative fluorescence intensity of these images was analyzed utilizing ImageJ image analysis software (NIH, Bethesda, MD, USA) (Hseu et al., 2018).

2.7. Detection of senescence-associated β-galactosidase activity

SA-β-Gal activity was carried out based on the modified method described by related researches (Han et al., 2017; Makpol et al., 2011). Cells were stained using the SA-β-Gal staining kit (Abbkine, Inc., Wuhan, China). The staining procedure was adhered to the manufacturer's protocol. Cell images were captured using a microscope at 400x magnification under three bright fields. The cells exhibiting blue-green stains were counted. The percentage of SA-β-Gal positive cells was determined by the ratio of stained cells to the total number of cells which indicates the presence of cellular senescence.

2.8. RNA-sequencing

Following the same cell culture procedure, cells were pre-treated with GRP and then exposed to UVA for 75 min. Afterward, the cells were harvested and RNA was extracted for subsequent experiments. The construction of the cDNA library and the sequencing analysis were carried out by BIOTOOLS Biotechnology Co., Ltd. (Taipei, Taiwan). High-throughput paired-end 150 bp sequencing was performed using the Illumina NovaSeq 6000 system (Illumina, San Diego, CA, U.S.A). The gene expression analysis was referenced from the Mus musculus-GRCm38 gene database and was calculated using feature counts. DEGs between each treatment group were identified using DESeq2, which ensured biological repeatability. The criteria for significant differential expression were set at a log2 fold change ≥2 and an adjusted p-value of ≤0.05. These parameters were applied in the GO analysis, as described by previous research (An et al., 2021; Farrukh et al., 2014).

2.9. Quantitative PCR (qPCR) analysis

RNA samples were reverse transcribed into cDNA by utilizing the GScript First Strand Synthesis Kit (GeneDireX, USA). Subsequently, quantitative PCR analysis was performed to amplify the promoter region of the DNA fragment. Specific primers were employed for the detection, as detailed in Table S1. To standardize the results, the relative abundance of housekeeping genes was exploited as the internal standard. Data regarding fold enrichment and the percentage of specific genes were collected and calculated (Chou and Ting, 2023).

2.10. ChIP analysis

After the treatments, the cells were incubated with 1 % formaldehyde at 37 °C to facilitate DNA–protein cross-linking. Then, glycine (125 mmol/L) was added to the cells and allowed to react for 5 min before transferring to lysis buffer. The cells were incubated overnight at 4 °C with Nrf2 antibodies in the presence of protease inhibitors, followed by washing with elution buffer. The cross-linked immunoprecipitated complexes were then incubated at 65 °C for 2 h. DNA fragments were subsequently purified using the ChIP DNA Clean & Concentrator Kit (Zymo, Tustin, CA, U.S.A), and quantitative PCR analysis was conducted to amplify the promoter regions of the GSR, SOD, and NQO1 genes using specific primers (as listed in Table S2) (Ryu et al., 2019; Tanigawa et al., 2007; Wang, Xu, et al., 2016). Data on the fold enrichment and percentage of specific genes in ChIP were collected and calculated according to the method described by previous researches (Harvey et al., 2009; Marionnet et al., 2010).

2.11. Lifespan assay and pharyngeal pumping

The method was adapted from previous research with modifications (Wang et al., 2020). Briefly, 30–50 L4 stage *C. elegans* N2 (Wild-type) were placed on NGM agar with *E. coli* OP50, 1 mmol/L NAC, and either 50 or 100 μg/mL GRP. The worms were cultured at 20 °C and periodically transferred to fresh agar every two days to maintain adequate food supply. They were monitored until death to determine their life spans. FudR-added NGM agar was used to inhibit reproduction. The procedures to determine pharyngeal pumping rate and the lifespan assay were obtained from previous research with slightly modifications (How et al., 2018). On the seventh day of the assay, a minimum of 20 worms were examined under a microscope to count their pharyngeal contractions per minute (pumps rate/min).

2.12. Stress resistance

The process to determine stress resistance was based on previous research with alterations: L1 stage *C. elegans* N2 (Wild-type) in M9 buffer were treated in a 96-well plate with *E. coli*, 1 mmol/L NAC, and either 50 or 100ug/mL GRP for 48 h. Post-treatment was carried out by adding 50 μL Juglone (250 μmol/L final concentration). Juglone was prepared by diluting a hundred folds of 50 mmol/L DMSO stock with M9 buffer. The survival rates were observed after 6 h (Shi et al., 2012).

2.13. Molecular docking simulation

The crystal structure of Keap1 (BTB domain) was retrieved from the Research Collaboratory for Structural Bioinformatics Protein Databank (Keap1-BTB; PDB entry: 4CXT). Utilizing AutoDockTools, all water molecules were removed from the receptor, and hydrogen atoms and Kollman charges were manually added to the structure, as detailed by previous research (Marionnet et al., 2010). Ligand structures were obtained from the PubChem database. Again, AutoDockTools was used to remove water molecules from the receptor. Hydrogen atoms and Gasteiger charges were then added to the ligands. A grid box with the dimension of 36 Å × 51 Å × 45 Å along the X-, Y-, and Z-axes was created to incorporate the Keap1-BTB protein structure, while the grid spacing was set at 0.375 Å. The grid center for Keap1-BTB was determined to be X = 5.043, Y = −9.302, and Z = −13.046. The docked conformations between Keap1-BTB and various compounds were ranked based on the predicted binding free energy (affinity) values, which are expressed in

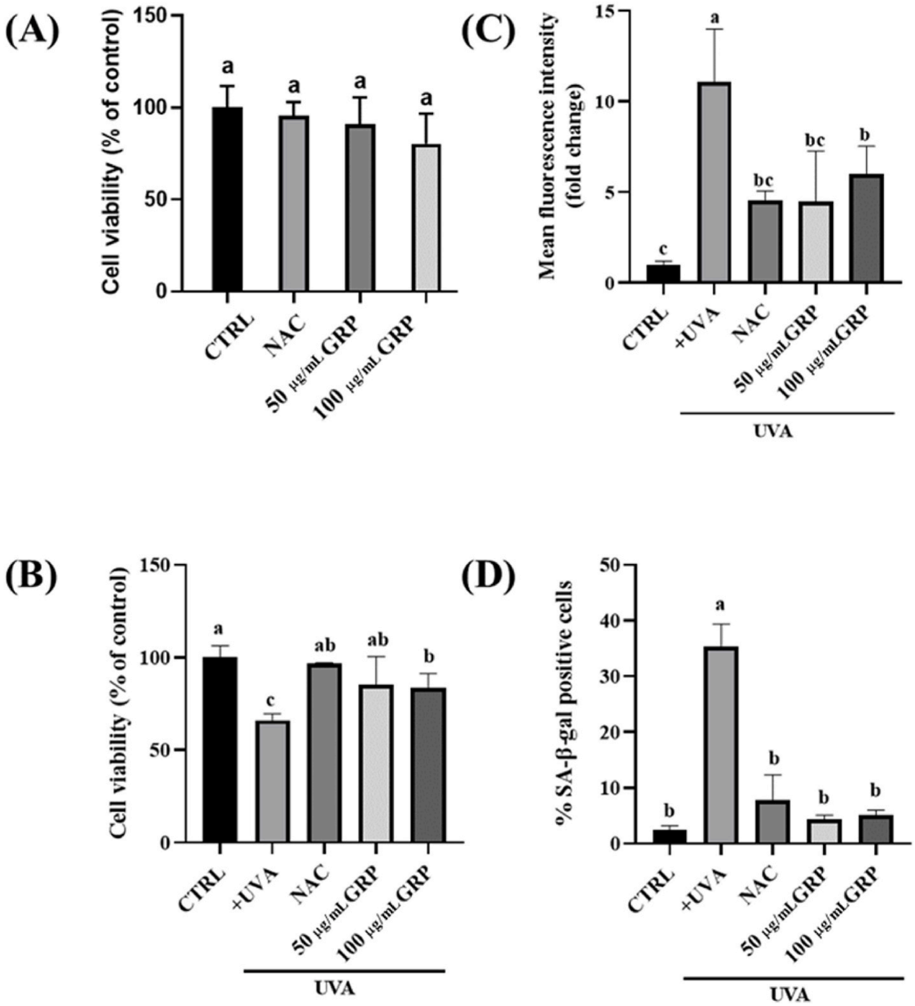

Fig. 1. Effect of GRP on SA-β-gal activity and ROS production in UVA irradiated Hs68 cells. (A) Cell viability at different doses of GRP treatment; (B) Cell viability at different doses of pretreated GRP with UVA irradiation; (C) Mean fluorescence intensity changes according to ImageJ software analysis; (D) Percentage of SA-β-gal positive cells compared to the total Hs68 cell numbers.

The experimental results were repeated three times, and all were expressed in the form of mean ± standard deviation (SD). Different letters indicate significant differences ($p < 0.05$).

CTRL: Without treatment; UVA: Being exposed to 15 kJ/cm^2 UVA; NAC: Pretreated with 1 mmol/L N-acetylcysteine before 15 kJ/cm^2 UVA-irradiation. GRP: Pretreated with 50 or 100ug/mL GRP before 15 kJ/cm^2 UVA-irradiation.

kcal/mol. The docking results for all compounds that interacted with Keap1-BTB were visualized using the Pymol software (Shi et al., 2012).

2.14. Statistical methodology

All experiments were performed in triplicate, and the resulting measurement values are presented as mean ± standard deviation. Statistical analysis were performed using IBM SPSS 20 (International Business Machines Co., New York, USA). The differences between mean values were assessed using analysis of variance, with Duncan's multiple range test for post-hoc comparisons. The p-value of less than 0.05 was deemed statistically significant.

3. Results and discussion

3.1. GRP modulates ROS production and prevents UVA-induced aging

As illustrated in Fig. 1A, different concentrations of GRP and 1 mmol/L NAC demonstrate minimal effects to cell viability, which indicates their biocompatibility. After inducing the cells with 15 J/cm^2 UVA irradiation, it can be observed that cells pretreated with NAC (1 mmol/L) and GRP at 50 μg/mL showed an increase in survival rate (Fig. 1B). Furthermore, 50 μg/mL GRP possesses a relatively similar modulating effect to NAC on the pretreated cells, suggesting that GRP may be able to alleviate oxidative stress induced by UVA. This highlights GRP's ability to attenuate damages from photoaging, as can be seen in Fig. 1C and S1A. Moreover, it can also help eliminate DNA-damaging ROS products such as hydrogen peroxide and lipid peroxides (Hsieh, Yu, Cheng, et al., 2023). In a study conducted by Rom et al. (2022), they found that glycine supplementation could enhance GSH production and reduce oxidative stress, thereby alleviating the pathogenesis of atherosclerosis (Rom et al., 2022). Given that GRP is rich in glycine and showing similar antioxidative effects to NAC, supplementation of GRP is speculated to enhance GSH activity, potentially delaying oxidative stress.

Yin and Jiang et al. (2013) reported that β-galactosidase activity in UVA-irradiated fibroblasts is activated in a dose-dependent manner (Yin & Jiang, 2013). By pretreating Hs68 cells with 1 mmol/L NAC as well as GRP at 50 μg/mL and 100 μg/mL, the senescence-associated (SA)-β-gal staining ratios were significantly reduced ($p < 0.05$) by 7.76 ± 4.61 %, 4.36 ± 0.75 %, and 5.06 ± 0.95 %, respectively (Fig. 1D and Fig. S1B). The reduction of cellular senescence indicator like SA-β-gal activity suggests GRP's ability in delaying photoaging. Similarly, the low molecular weight peptides (458 Da) from *Agaricus blazei* also demonstrate a dose-dependent reduction of SA-β-gal-positive cells in a D-galactose-induced senescence model (Feng et al., 2022). These findings imply GRP's potential in combating against non-replicative aging by reducing oxidative stress, which is comparable to other natural health products derived from food.

3.2. Possible mechanism regulated by GRP according to transcriptomic analysis

UV radiation can damage gene expression patterns, altering differential DEGs. After UVA exposure, 2175 DEGs from Hs68 cells were upregulated while 3257 were downregulated. On the other hand, when the cells were pretreated with 100 μg/mL GRP prior to UVA exposure, 494 genes were upregulated, and 655 genes were downregulated, as can be observed in Fig. S2 A and B. These numbers reveal notable differences of gene expression between the experimental groups. Through the bioinformatics database Gene Ontology (GO), variations between groups and genes involved were examined which focused on biological effects and mechanisms within Hs68 cells during GRP pretreatment and after UVA exposure (Thomas et al., 2019). The DEGs, both upregulated and downregulated, underwent GO analysis for functional categorization. Compared to the non-irradiated control group, the UVA-induced group experiences significant upregulation from oxidative stress (Fig. 2A) and reduction in the negative regulation of the cell cycle (Fig. 2B). Conversely, the group pretreated with GRP before UVA exposure shows noticeable downregulation in response to oxidative stress (Fig. 2C) and elevation in the positive regulation of cell cycle (Fig. 2D). The analysis from QuickGO (https://www.ebi.ac.uk/QuickGO/) reveals that the response to oxidative stress (GO:0006979) and regulation of cell cycle (GO:0051726) are categorized under Biological Process. Moreover, as shown in Fig. S2 C, D, post-GRP treatment leads to further downregulation after subjecting the cells to UVA, in addition to an improvement in the positive regulation of the cell cycle (GO:0045787). Thus, GRP can delay cellular aging.

Exposure to 3 J/cm^2 UVA increases oxidative stress by 4 folds which can induce collagen degradation and phosphorylation of c-Fos, c-Jun, and NF-κB in Hs68 cells [17]. In addition, discovered that exposure to 10 J/cm^2 UV results in *p*53 mRNA translation and homo-oligomerization in Hs68 cells, leading to G2/M phase arrest (Farrukh et al., 2014). Hence, even UV radiation at low exposure can instigate responses of many transcription factors to alter gene expression. ROS play a crucial role in cellular senescence by activating stress-induced signaling pathways, including MAPK/ERK and PI3K/Akt, which regulate apoptosis and inflammatory responses (Albanesi et al., 2023; Odawara et al., 2024). In particular, excessive ROS production impairs mitochondrial function, leading to a decline in ATP production and increased oxidative damage to lipids, proteins, and DNA (Lebiedzinska-Arciszewska et al., 2024; Li et al., 2022). These effects collectively contribute to non-replicative aging by disrupting cellular homeostasis and promoting SASP expression (Mahmud et al., 2024). Functional enrichment analysis revealed that GRP treatment at 100 μg/mL significantly reduces ($p < 0.05$) intracellular ROS levels by 33 % while modulating the phosphorylation and nuclear translocation of NF-κB (Hsieh, Yu, Cheng, et al., 2023). Furthermore, previous studies have demonstrated that bioactive peptides from fermented sources can activate the Nrf2/Keap1 signaling pathway, thereby upregulating phase II detoxification enzymes and mitigating oxidative damage, given the role of ROS in perpetuating cellular senescence (Lin et al., 2024). Consequently, the method can provide insights into the biological pathways and offer predictions for overall regulatory mechanisms. According to the gene functional enrichment analysis, it is hypothesized that GRP may regulate oxidative stress pathways, altering cell cycle arrest and thereby providing protection against photoaging.

3.3. Enhancing Nrf2 pathway and reducing oxidative stress in counteracting non-replicative aging

Under an oxidative stress condition, the Nrf2 pathway is activated which facilitates the translocation of Nrf2 into the nucleus to bind with antioxidative genes [25]. The interaction results in the production of enzymes, such as HO-1 and NQO1, to alleviate oxidative stress. This finding is highlighted in Ahmed et al. (2017) as it shows the potential of antioxidants in delaying aging (Ahmed et al., 2017). Meanwhile, this study compared the untreated and 100 μg/mL GRP-pretreated cells under UVA radiation (15 J/cm^2). Based on Fig. 3A and B, the pretreated cells exhibited a significant increase ($p < 0.05$) in the expression levels of *Nrf2* (3.86 times) and *HO-1* (2.32 times). The finding aligns with Chu et al. (2016) as they reported that *C. formosanum* extract can activate the Nrf2/HO-1 pathway in Hs68 cells, protecting cells against UV-induced photoaging by upregulating *Nrf2* and *HO-1* expression (Chu et al., 2016). Furthermore, GRP pretreatment at 100 μg/mL significantly decreased *p53* and *p21* expressions by 2.81 and 0.23 folds, respectively, compared to control (Fig. 3C and D). The results from this research study are similar to those found in Chen et al. (2019) as they employed ChIP assays and reported that 1,25-dihydroxyvitamin D3 in natural substances can inhibit ROS production by upregulating the Nrf2 transcription factor (Chen et al., 2019). The upregulation of Nrf2 reduces DNA damage and suppresses *p53* and *p21* gene expression, contributing to the

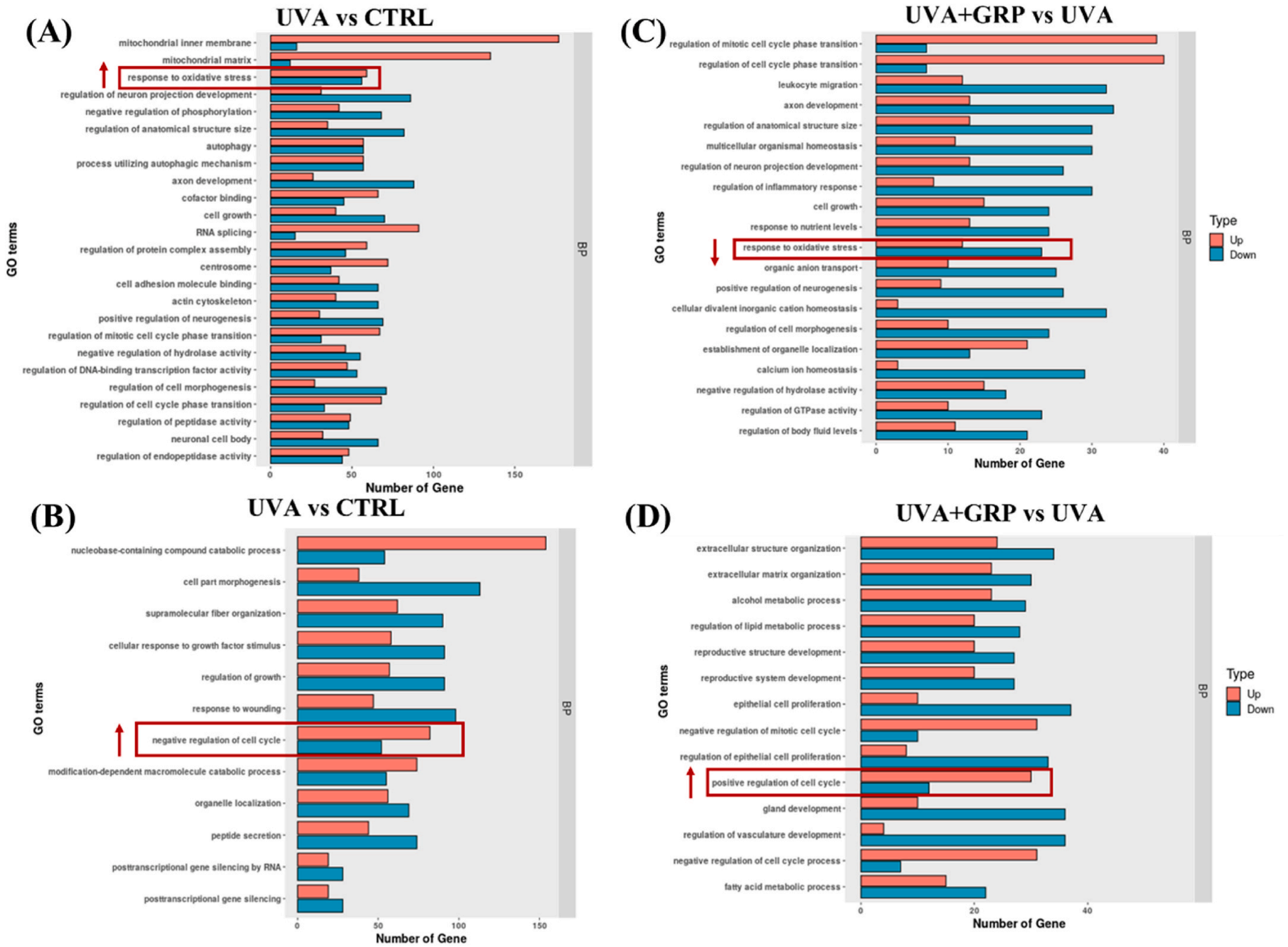

Fig. 2. Gene Ontology (GO) enrichment analysis. (A) UVA vs CTRL groups upregulate responses to oxidative stress; (B) UVA vs CTRL groups modulate the negative cell cycle process; (C) UVA + GRP vs UVA groups downregulate responses to oxidative stress; (D) UVA + GRP vs UVA groups modulate the positive cell cycle process.

BP: Biological process; CTRL: Without treatment; UVA: Being exposed to 15 kJ/cm^2 UVA; NAC: Pretreated with 1 mmol/L N-acetylcysteine before 15 kJ/cm^2 UVA-irradiation. GRP: Pretreated with 50 or 100ug/mL GRP before 15 kJ/cm^2 UVA-irradiation.

delay in cellular aging (Chen et al., 2019). Proteins such as p53 and p21 are identified as inhibitors of cyclin-dependent kinases which can activate senescent cells and arrest them in the G0/G1 phase of cell cycle (Sasaki et al., 2014). These findings emphasize the functions of antioxidants in natural foods for combating cellular aging: They may play a vital role in the enhancement of Nrf2 transcription factor and the activation of ARE.

In addition, Nrf2 activation has been observed to protect cells from oxidative stress by stimulating the expression of key antioxidant enzymes, including SOD, GSR, and NQO1 (Duangjan et al., 2019; Hsieh et al., 2024; Tang et al., 2021). Moreover, Nrf2 plays a crucial role in modulating DNA-protein interactions essential for cellular homeostasis, particularly by regulating gene transcription involved in detoxification and oxidative stress response. This regulatory mechanism is vital for the expression of genes responsible for maintaining redox balance and mitigating oxidative damage. Nrf2 exerts its protective function by binding to antioxidant response elements (AREs) in the promoter regions of target genes, thereby facilitating their transcription and enhancing cellular resilience against oxidative insults (Das et al., 2004; Lopez-Ruiz et al., 2023; Wu et al., 2023). After UVA exposure, the groups pretreated with 50 and 100 μg/mL GRP were observed to have expression upregulation in *GSR* (1.33 and 2.75 times), *SOD* (1.44 and 1.86 times), and *NQO1* (2.27 and 2.49 times) compared to the untreated group with statistically significant differences ($p < 0.05$) (Fig. 3E, F, and G). It can be concluded that GRP reduces oxidative stress induced by UVA through the induction of Nrf2 pathway which suppresses the manifestation of non-replicative aging.

3.4. Effects of GRP on lifespan extension and stress resistance in C. elegans

GRP was pretreated on *C. elegans* to determine its role in extending lifespan and improving stress resistance on the organisms. Fig. 4A demonstrates that the survival curves of GRP- and NAC-treated *C. elegans* exhibit a rightward shift. Compared to the control group, the average lifespan increases by 9.7 ± 2.0 % for NAC, 13.4 ± 3.8 % for 50 μg/mL GRP, and 11.0 ± 2.8 % for 100 μg/mL (Table 1). In another study, peptides from sesame at 50 μg/mL were shown to extend the average lifespan of *C. elegans* by 5.2 %, demonstrating the anti-aging potential of peptides found in natural foods (Wang, Ma, et al., 2016). On the other hand, Oh et al. (2015) reported that an addition of NAC to *C. elegans*' diet can extend the average lifespan by 28.1 % (Oh et al., 2015). This may be attributed to the enhanced resistance to oxidative stress, heat stress, and UV radiation.

In addition to the average life span, pharyngeal pumping rate of *C. elegans* may also serve as another biological marker associated with

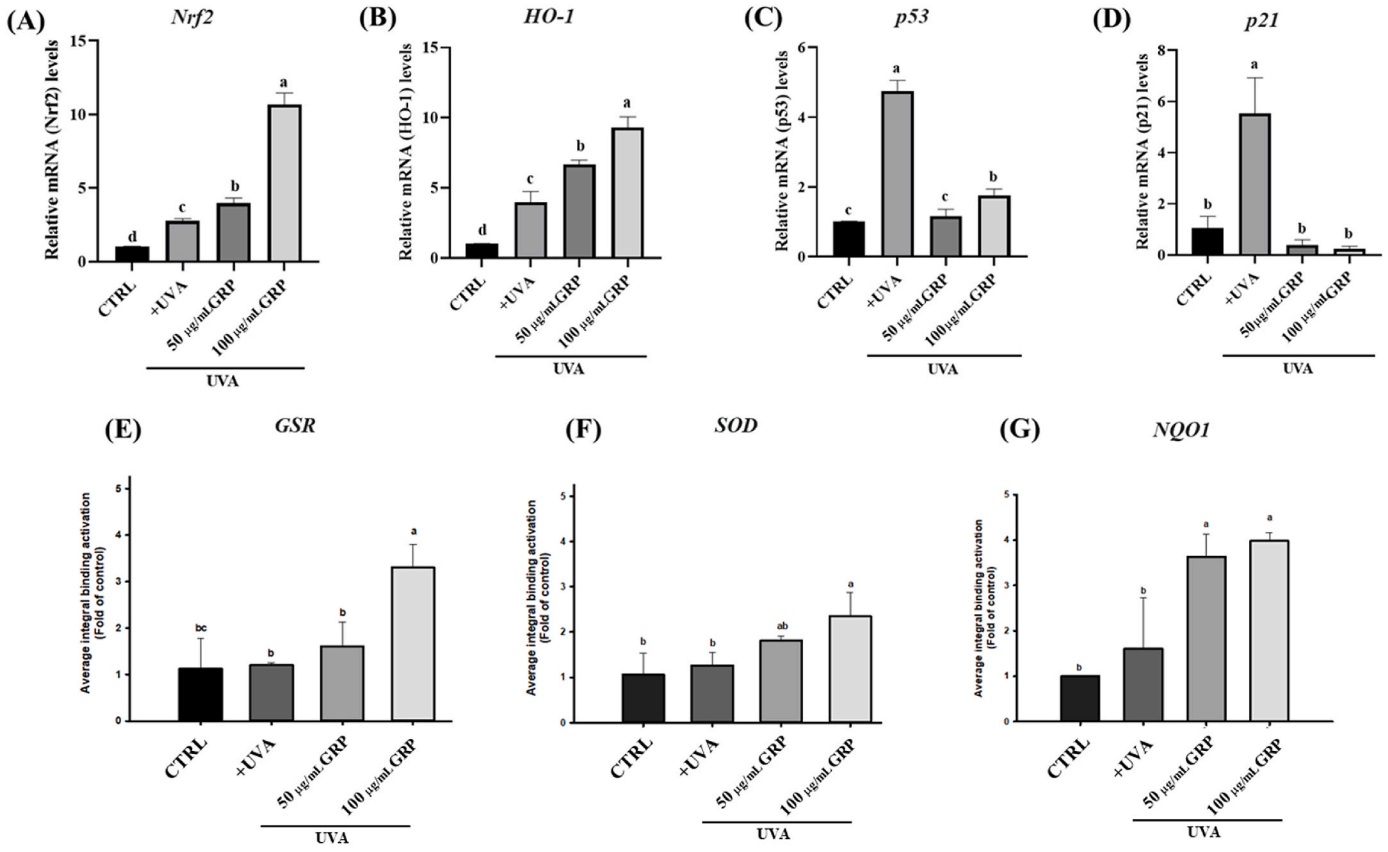

Fig. 3. Effect of GRP on gene expressions (A to D) and ChIP analysis of irradiated cells (E to G). (A) *Nrf2*; (B) *HO-1*; (C) *p53*; (D) *p21*; (E) *GSR*; (F) *SOD*; (G) *NQO1*.

The experimental results were repeated three times, and all were expressed in the form of mean ± standard deviation (SD). Different letters indicate significant differences ($p < 0.05$).

CTRL: Without treatment; UVA: Being exposed to 15 kJ/cm^2 UVA; GRP: Pretreated with 50 or 100ug/mL GRP before 15 kJ/cm^2 UVA-irradiation.

worm aging (Chiu et al., 2018). Pharyngeal pumping rate could be investigated to assess health which is correlated to the remaining lifespan (Bansal et al., 2015). On Day 7, the pharyngeal pumping rates of *C. elegans* after treating with NAC and GRP (at 50 and 100 μg/mL) were 280 ± 4, 223 ± 11, and 276 ± 8 pumps/min, respectively, compared to 203 ± 10 pumps/min in the control group (Fig. 4B). Additionally, juglone was exploited to induce oxidative stress in *C. elegans* (Moliner et al., 2019). It was found that the addition of NAC, 50 μg/mL GRP, and 100 μg/mL GRP can significantly enhance the survival rate of *C. elegans* by 98.5 ± 0.1 %, 80.4 ± 0.1 %, and 80.6 ± 2.4 %, respectively, compared to the control group ($p < 0.05$) (Fig. 4C). This finding indicates the capability of GRP as a worm supplement to enhance resistance to oxidative stress. Further testing under oxidative stress revealed that both 50 and 100 μg/mL treated-GRP promote gene expression of *skn-1* (1.67, 1.70 times), *gcs-1* (2.87, 5.75 times), *gst-4* (1.44, 1.86 times), and *gst-7* (3.01, 3.99 times) compared to the juglone-treated group with statistically significant differences ($p < 0.05$), as illustrated in Fig. 4D, E, F, and G. The transcription factor SKN-1, when exposed to juglone, moves to the nucleus and activates the expression of multiple detoxification genes (Kahn et al., 2007; Wu et al., 2016). SKN-1 induces the expression of phase II detoxification genes, such as gcs-1 and trx-1, which are essential for oxidative stress resistance (Hwang et al., 2022). Activation or overexpression of *skn-1* activate the SKN-1/Nrf2 pathway, leading to upregulation of antioxidant genes, reduced ROS accumulation, and prolonged lifespan in *C. elegans*, while the loss of this transcription factor may have an opposite effect (An et al., 2005; Kell et al., 2007; Tao et al., 2023). This study illustrates that GRP increases gene expression of *skn-1*, which can subsequently be hypothesized that the increased activity of SKN-1 reduces endogenous ROS through nuclear translocation (Fig. 4D). Similarly, high hydrophobic amino acids content peptides similar to GRP that was extracted from *Phalaris canariensis* also triggers an overexpression of *gst-4* gene in *C. elegans*, implying its potential as a natural antioxidant in foods (Urbizo-Reyes et al., 2022). Thus, a mechanism of GRP in increasing lifespan and improving stress resistance in *C. elegans* is speculated.

3.5. Molecular interactions and inhibitory OGT mechanisms of GTP on the Keap-BTB

As mentioned previously, Nrf2 transcription factor regulates gene expression that is responsible in modulating ROS. On top of that, Keap1 protein is a negative regulator Nrf2, whereby BTB domain on Keap1 is the inhibitory site (Chen et al., 2017; Xu et al., 2022). By simulating the molecular interaction of GRP peptide, it is hypothesized that the peptide targets and binds to the Keap1-BTB inhibitory site, creating a docking affinity of −5.22 kcal/mol. Based on Fig. 5, GRP forms four hydrogen bonds with Ser102, Ser103, and Ser166, where their bond lengths are measured to be between 2.98 and 3.21 Å. The first three glycine residues in the GRP peptide predominantly form these hydrogen bonds. Additionally, GRP's glycine residues and Ser104, Pro105, Phe139, Gln163, Ile164, and Asp165 also create covalent bonding. The molecular docking results suggest that the distinctive repetitive glycine structure in GRP confers an inhibitory effect on Keap1-BTB. Furthermore, lysine and proline residues of the GRP peptide are found to covalently bond at the Keap1-BTB inhibitory pocket, specifically at Thr60, Phe64, Ala140, Tyr141, Thr142, and Ala143 (Fig. 5).

Protein glycosylation is one of the most common post-translational modifications in mammals. Within the context of Keap1, its

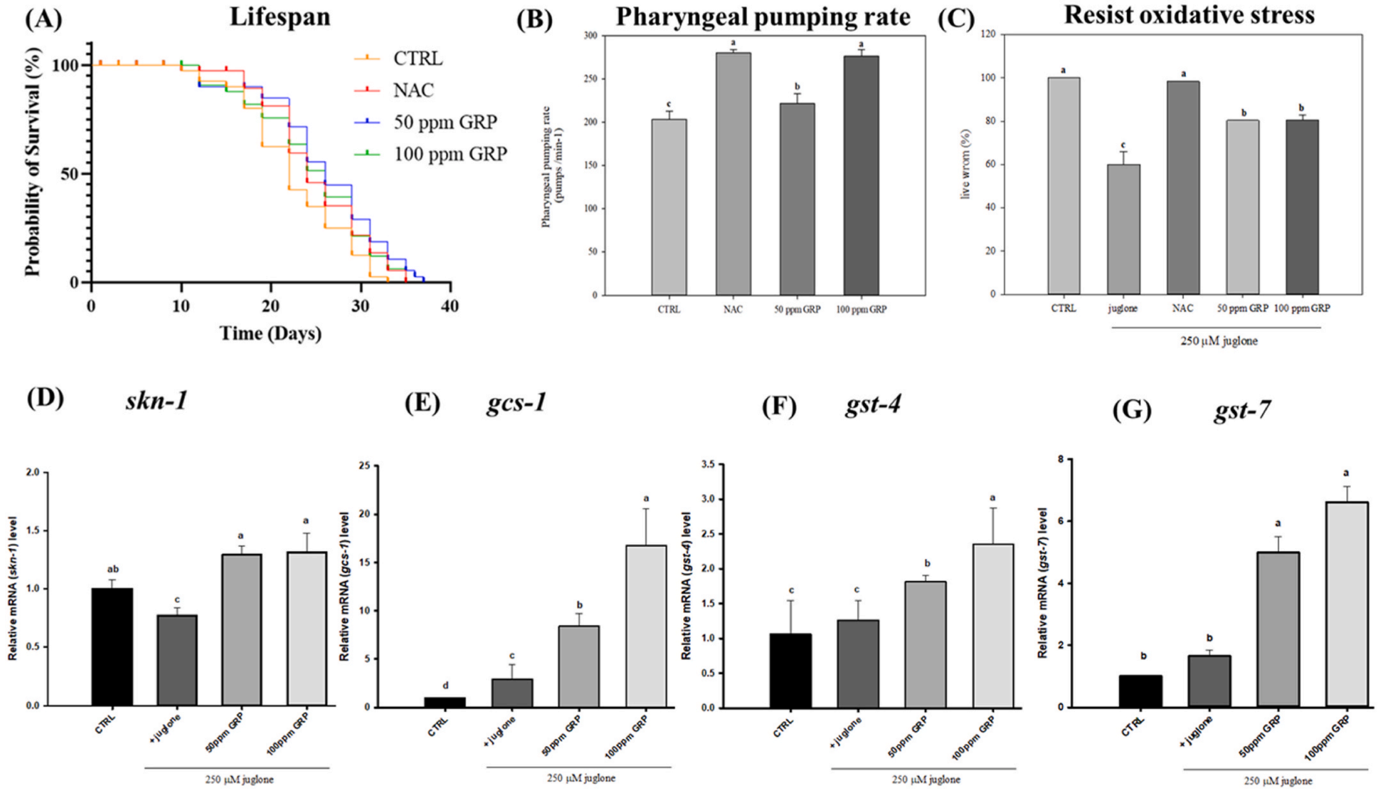

Fig. 4. Effect of different treatments on N2 wild-type *C. elegans*. (A) Lifespan study; (B) Pharyngeal pumping rate; (C) Resistance to oxidative stress; (D) *skn-1* gene expression; (E) *gcs-1* gene expression; (F) *gst-4* gene expression; (G) *gst-7* gene expression.

The experimental results were repeated three times, and all were expressed in the form of mean ± standard deviation (SD). Different letters indicate significant differences ($p < 0.05$).

CTRL: Without treatment; Juglone: Treated with 250 μM Juglone; NAC: Treated with 1 mmol/L N-acetylcysteine supplement; GRP: Treated with 50 or 100 μg/mL of GRP.

Table 1
Effect of GRP on the mean lifespan of N2 wild-type *C. elegans*.

Group	Mean lifespan	% of control
CTRL	22.8 ± 0.58^{b}	100.0 ± 2.54^{b}
1 mmol/L NAC	25.0 ± 0.46^{a}	109.7 ± 2.02^{a}
50 μg/mL GRP	25.82 ± 0.86^{a}	113.4 ± 3.78^{a}
100 μg/mL GRP	25.26 ± 0.63^{a}	111.0 ± 2.77^{a}

The experimental results were repeated three times, and all were expressed in the form of mean ± standard deviation (SD). Different letters indicate significant differences ($p < 0.05$).

CTRL: Without treatment, CTRL: Without treatment; NAC: Treated with 1 mmol/L NAC supplement; GRP: Treated with 50 or 100 μg/mL GRP.

glycosylation depends on the activity of a single OGT (Mehboob and Lang, 2021). Keap1 is found to physically interact with OGT at 11 alternative glycosylation sites which are located in different domains of Keap1. Key sites within the α-helices of the BTB domain, such as Ser104, Ser102, Ser103, and Ser166, are essential for Keap1 homodimerization and its interaction with CUL3 (Chen et al., 2018). When Keap1 is glycosylated by OGT, it triggers an inhibition of Nrf2. Therefore, the inhibition of OGT would effectively reduce the assembly of Keap1 in the Cul3-dependent ubiquitin ligase complex, activating the Nrf2 protein to enter the nucleus and stimulate the transcription of antioxidant response genes (How et al., 2018; Wang et al., 2020).

This interaction then decreases the Nrf2-KEAP complex state which enhances the translocation of Nrf2 into the nucleus. Consequently, Nrf2 could bind with ARE upon entering the nucleus and facilitate anti-oxidative mechanisms.

4. Conclusions

The comprehensive analysis of glycine-rich peptides from tempeh-like fermented *C. formosanum* reveals their significant role in combating oxidative stress and delaying photoaging. By comparing to NAC, GRP exhibits similar protective effects in enhancing cell survival after UVA irradiation. This is achieved by regulating gene expression of cell cycle and modulating oxidative stress responses. Furthermore, in vivo studies showed that GRP extends the lifespan of *C. elegans* and enhances their resistance to oxidative stress, underscoring its potential as a dietary supplement for health span extension. Additionally, molecular docking investigation identified GRP's potential mechanism as the inhibitor of OGT at the KEAP-BTB inhibitory site, thereby enhancing the Nrf2 pathway. These findings suggest that GRP, with its anti-oxidative properties, could serve as an effective natural intervention in delaying non-replicative aging and mitigating the effects of environmental stressors.

CRediT authorship contribution statement

Chen-Che Hsieh: Writing – original draft, Conceptualization. **Hui-Wen Lin:** Writing – original draft, Conceptualization. **Hsiao-Chu Huang:** Formal analysis, Data curation. **Darin Khumsupan:** Formal analysis, Data curation. **Szu-Chuan Shen:** Formal analysis, Data curation. **Shin-Ping Lin:** Formal analysis, Data curation. **Chang-Wei Hsieh:** Resources, Formal analysis. **Tsung-Yu Tsai:** Resources, Formal analysis. **Sirima Suvarnakuta Jantama:** Resources, Formal analysis. **Hsing-Chun Kuo:** Writing – review & editing, Supervision, Project administration, Funding acquisition, Conceptualization. **Kuan-Chen Cheng:**

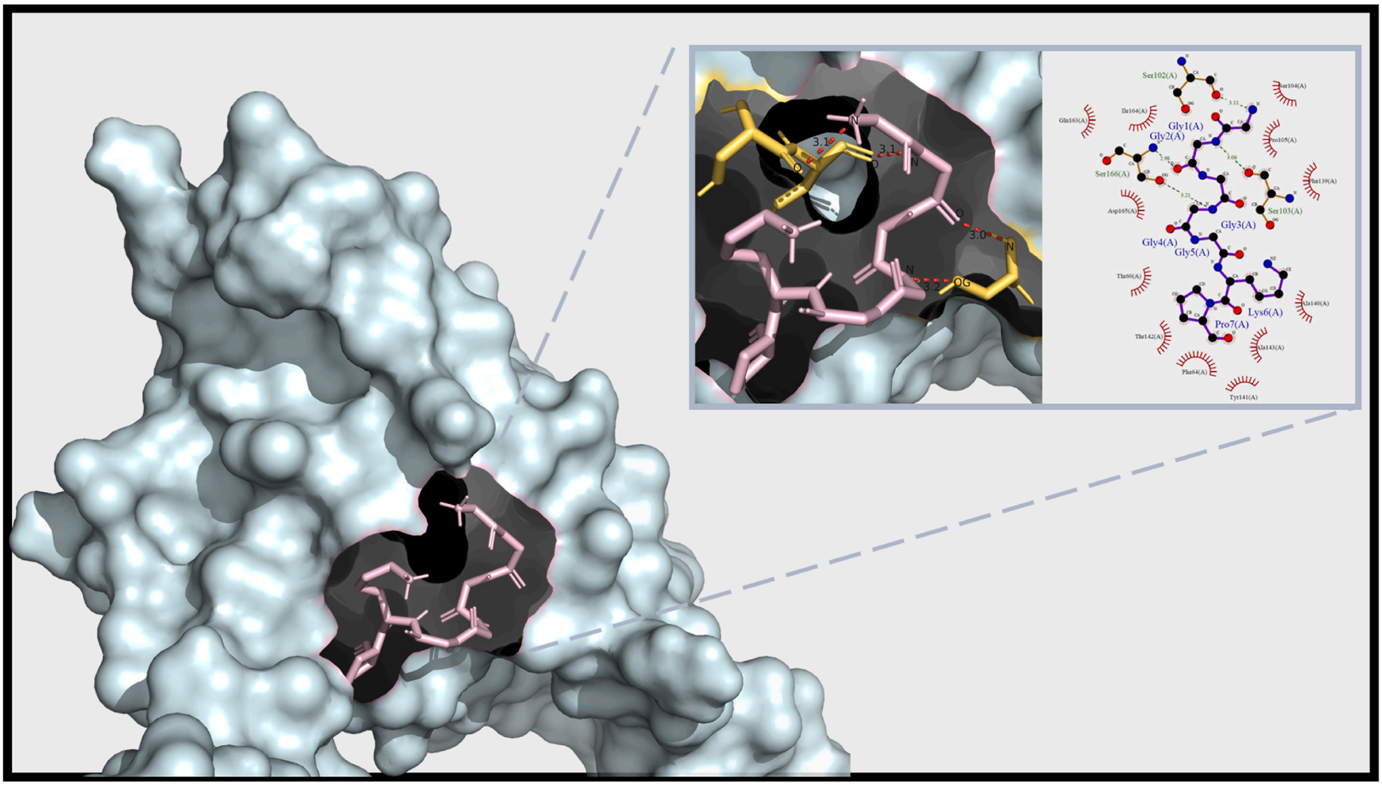

Fig. 5. The inhibition of Keap1-BTB by a glycine-rich peptide (GRP) obtained from tempeh-like fermented *Chenopodium formosanum*.

Writing – review & editing, Supervision, Project administration, Funding acquisition, Conceptualization.

Declaration of competing interest

I have nothing to declare.

Acknowledgments

The Funding for this study was provided in part by research grants from the Chang Gung Memorial Hospital, Chiayi, Taiwan. This study was supported by grants BMRPD42, CMRPF6M0071, CMRPF6M0072, CMRPF6M0073 and ZRRPF6P0011 from Chang Gung Memorial Hospital, Chiayi, Taiwan, and Chang Gung University of Science and Technology, Chiayi Campus, Taiwan. This work was supported by grants NSTC 112-2320-B-002-013-MY3; 112-2221-E-002-040-MY3; 113-2320-B-255-001-; 113-2222-E-992 -009 -MY2 from the National Science and Technology Council (NSTC), R.O.C. National Core Facility for Biopharmaceuticals, NSTC, particularly *C. elegans* Core Facility, for assistance.

Appendix A. Supplementary data

Supplementary data to this article can be found online at https://doi.org/10.1016/j.lwt.2025.117641.

Data availability

Data will be made available on request.

References

Ahmed, A. S. I., Sheng, M. H., Wasnik, S., Baylink, D. J., & Lau, K. H. W. (2017). Effect of aging on stem cells. *World Journal of Experimental Medicine, 7*, 1. https://doi.org/10.5493/wjem.v7.i1.1

Albanesi, C., Mercurio, L., Bailey, J., Glick, A., Dellambra, E., Scarponi, C., & Madonna, S. (2023). RAS-activated PI3K/AKT signaling sustains cellular senescence in experimental models of psoriasis via P53/P21 axis. https://doi.org/10.21203/rs.3.rs-3209194/v1.

An, J. H., Vranas, K., Lucke, M., Inoue, H., Hisamoto, N., Matsumoto, K., & Blackwell, T. K. (2005). Regulation of the *Caenorhabditis elegans* oxidative stress defense protein SKN-1 by glycogen synthase kinase-3. *Proceedings of the National Academy of Sciences, 102*, 16275–16280. https://doi.org/10.1073/pnas.0508105102

An, J., Zhang, S., Xia, X., Dong, Z., Zhou, W., Mai, W., & Jin, D. (2021). Transcriptomics changes and the candidate pathway in human macrophages induced by different PM2.5 extracts. *Environmental Pollution, 289*, Article 117890. https://doi.org/10.1016/j.envpol.2021.117890

Bansal, A., Zhu, L. J., Yen, K., & Tissenbaum, H. A. (2015). Uncoupling lifespan and healthspan in *Caenorhabditis elegans* longevity mutants. *Proceedings of the National Academy of Sciences, 112*, E277–E286. https://doi.org/10.1073/pnas.1412192112

Bao, T., Wang, Y., Li, Y. T., Gowd, V., Niu, X. H., Yang, H. Y., & Chen, W. (2016). Antioxidant and antidiabetic properties of tartary buckwheat rice flavonoids after in vitro digestion. *Journal of Zhejiang University - Science B, 17*, 941. https://doi.org/10.1631/jzus.B1600243

Chen, P. H., Ho, P. C., Tsui, Y. C., Lin, C. H., Chi, J. T., & Boyce, M. (2018). Functional crosstalk among oxidative stress and O-GlcNAc signaling pathways. *Glycobiology, 28*, 556–564. https://doi.org/10.1093/glycob/cwy027

Chen, P. H., Smith, T. J., Wu, J., Siesser, P. F., Bisnett, B. J., Khan, F., Hogue, M., Lin, Z., Mayo, L. D., Jelinek, D. F., Chi, J. T., & Boyce, M. (2017). Glycosylation of KEAP1 links nutrient sensing to redox stress signaling. *The EMBO Journal, 36*, 2233–2250. https://doi.org/10.15252/embj.201696113

Chen, L., Yang, R., Qiao, W., Zhang, W., Chen, J., Mao, L., & Miao, D. (2019). 1,25-Dihydroxyvitamin D exerts an antiaging role by activation of Nrf2-antioxidant signaling and inactivation of p16/p53-senescence signaling. *Aging Cell, 18*, Article e12951. https://doi.org/10.1111/acel.12951

Chen, W., Zhuang, J., Li, Y., Shen, Y., & Zheng, X. (2013). Myricitrin protects against peroxynitrite-mediated DNA damage and cytotoxicity in astrocytes. *Food Chemistry, 141*, 927–933. https://doi.org/10.1016/j.foodchem.2013.04.033

Chiu, H. F., Chen, T. J., Lu, Y. Y., Han, Y. C., Shen, Y. C., Venkatakrishnan, K., Golovinskaia, O., & Wang, C. K. (2018). Efficacy of protein rich pearl powder on antioxidant status in a randomized placebo-controlled trial. *Journal of Food and Drug Analysis, 26*, 309–317. https://doi.org/10.1016/j.jfda.2017.05.010

Chou, Y. J., & Ting, Y. (2023). Plasma-activated water regulated transcriptome gene expression leading to high germination and growth of mung beans. *Chemical and Biological Technologies in Agriculture, 10*, 146. https://doi.org/10.1186/s40538-023-00497-2

Chu, C. C., Chen, S. Y., Chyau, C. C., Fu, Z. H., Liu, C. C., & Duh, P. D. (2016). Protective effect of Djulis (*Chenopodium formosanum*) and its bioactive compounds against carbon tetrachloride-induced liver injury, in vivo. *Journal of Functional Foods, 26*, 585–597. https://doi.org/10.1016/j.jff.2016.08.025

Das, P. M., Ramachandran, K., vanWert, J., & Singal, R. (2004). Chromatin immunoprecipitation assay. *Biotechnology, 37*, 961–969. https://doi.org/10.2144/04376RV01

Duangjan, C., Rangsinth, P., Gu, X., Zhang, S., Wink, M., & Tencomnao, T. (2019). Glochidion zeylanicum leaf extracts exhibit lifespan extending and oxidative stress resistance properties in *Caenorhabditis elegans* via DAF-16/FoxO and SKN-1/Nrf-2 signaling pathways. *Phytomedicine, 64*, Article 153061. https://doi.org/10.1016/j.phymed.2019.153061

Farrukh, M. R., Saeed, M., & Ahmad, I. (2014). Oxidative stress mediated Ca2+ release manifests endoplasmic reticulum stress leading to unfolded protein response in UV-B irradiated human skin cells. *Journal of Dermatological Science, 75*, 24–35. https://doi.org/10.1016/j.jdermsci.2014.03.005

Feng, Q., Lu, X., Yuan, G., Zhang, Q., & An, L. (2022). Effects of Agaricus blazei polypeptide on cell senescence by regulation of Keap1/Nrf2/ARE and TLR4/NF-κB p65 signaling pathways and its mechanism in D-gal-induced NIH/3T3 cells. *Journal of Functional Foods, 72*, Article 104037. https://doi.org/10.1016/j.jff.2020.104037

Fu, P. P., Xia, Q., Hwang, H. M., Ray, P. C., & Yu, H. (2014). Mechanisms of nanotoxicity: Generation of reactive oxygen species. *Journal of Food and Drug Analysis, 22*, 64–75. https://doi.org/10.1016/j.jfda.2014.01.005

Guo, H., Hao, Y., Yang, X., Ren, G., & Richel, A. (2023). Exploration on bioactive properties of quinoa protein hydrolysate and peptides: A review. *Critical Reviews in Food Science and Nutrition, 63*, 2896–2909. https://doi.org/10.1080/10408398.2021.1982860

Han, B. I., Hwang, S. H., & Lee, M. A. (2017). A progressive reduction in autophagic capacity contributes to induction of replicative senescence in Hs68 cells. *The International Journal of Biochemistry & Cell Biology, 92*, 18–25. https://doi.org/10.1016/j.biocel.2017.09.005

Harvey, C. J., Thimmulappa, R. K., Singh, A., Blake, D. J., Ling, G., Wakabayashi, N., Fujii, J., Myers, A., Biswal, S., Sporn, M. B., Liby, K. T., & Kensler, T. W. (2009). Nrf2-regulated glutathione recycling independent of biosynthesis is critical for cell survival during oxidative stress. *Free Radical Biology and Medicine, 46*, 443–453. https://doi.org/10.1016/j.freeradbiomed.2008.10.040

How, C. M., Li, S. W., & Liao, V. H. C. (2018). Chronic exposure to triadimenol at environmentally relevant concentration adversely affects aging biomarkers in *Caenorhabditis elegans* associated with insulin/IGF-1 signaling pathway. *The Science of the Total Environment, 640*, 485–492. https://doi.org/10.1016/j.scitotenv.2018.05.314

Hseu, Y. C., Kumar, K. J. S., Chen, C. S., Chen, S. C., Huang, H. C., Wang, H. M., Lin, C. M., & Lee, H. Z. (2018). Trans-cinnamic acid attenuates UVA-induced photoaging through inhibition of AP-1 activation and induction of Nrf2-mediated antioxidant genes in human skin fibroblasts. *Journal of Dermatological Science, 90*, 123–134. https://doi.org/10.1016/j.jdermsci.2018.01.004

Hsiao, Y. F., Chen, Y. C., Lai, Y. C., Chen, H. Y., & Tsai, P. J. (2023). Physicochemical properties and protective effects on UVA-induced photoaging in Hs68 cells of Pleurotus ostreatus polysaccharides by fractional precipitation. *International Journal of Biological Macromolecules, 228*, 537–547. https://doi.org/10.1016/j.ijbiomac.2022.12.254

Hsieh, C. C., Yu, S. H., Cheng, K. W., Liou, Y. W., Hsu, C. C., Hsieh, C. W., & Cheng, K. C. (2023). Production and analysis of metabolites from solid-state fermentation of *Chenopodium formosanum* (Djulis) sprouts in a bioreactor. *Food Research International, 168*, Article 112707. https://doi.org/10.1016/j.foodres.2023.112707

Hsieh, C. C., Yu, S. H., Kuo, H. C., Cheng, K. W., Hsu, C. C., Lin, Y. P., & Cheng, K. C. (2024). Alleviation of PM2.5-induced alveolar macrophage inflammation using extract of fermented *Chenopodium formosanum* Koidz sprouts via regulation of NF-κB pathway. *Journal of Ethnopharmacology, 318*, Article 116980. https://doi.org/10.1016/j.jep.2023.116980

Hsieh, C. C., Yu, S. H., Kuo, H. C., Khumsupan, D., Huang, H. C., Liou, Y. W., & Cheng, K. C. (2023). Glycine-rich peptides from fermented *Chenopodium formosanum* sprout as an antioxidant to modulate the oxidative stress. *Journal of Food and Drug Analysis, 31*, 5. https://doi.org/10.38212/2224-6614.3476

Huang, A. H., & Chien, A. L. (2020). Photoaging: A review of current literature. *Current Dermatology Reports, 9*, 22–29. https://doi.org/10.1007/s13671-020-00288-0

Hwang, M., Shrestha, C., Kang, S., & Kim, J. (2022). MEKK-3 acts cooperatively with NSY-1 in SKN-1-Dependent manner against oxidative stress and aging in *Caenorhabditis elegans*. *Biology, 11*(10), 1526. https://doi.org/10.3390/biology11101526

Kahn, N. W., Rea, S. L., Moyle, S., Kell, A., & Johnson, T. E. (2007). Proteasomal dysfunction activates the transcription factor SKN-1 and produces a selective oxidative-stress response in *Caenorhabditis elegans*. *Biochemical Journal, 409*, 205–213. https://doi.org/10.1042/BJ20070521

Kell, A., Ventura, N., Kahn, N., & Johnson, T. E. (2007). Activation of SKN-1 by novel kinases in *Caenorhabditis elegans*. *Free Radical Biology and Medicine, 43*, 1560–1566. https://doi.org/10.1016/j.freeradbiomed.2007.08.025

Kuo, H. C., Kwong, H. K., Chen, H. Y., Hsu, H. Y., Yu, S. H., Hsieh, C. W., & Cheng, K. C. (2021). Enhanced antioxidant activity of *Chenopodium formosanum* koidz. By lactic acid bacteria: Optimization of fermentation conditions. *PLoS One, 16*, Article e0249250. https://doi.org/10.1371/journal.pone.0249250

Lebiedzinska-Arciszewska, M., Suski, J., Bonora, M., Pakula, B., Pinton, P., Duszynski, J., & Wieckowski, M. R. (2024). The relation between mitochondrial membrane potential and reactive oxygen species formation. In *In mitochondrial bioenergetics: Methods and protocols* (pp. 133–162). New York, NY: Springer US. https://doi.org/10.1007/978-1-0716-4264-1_8.

Lee, J. Y., Yoo, D. G., Jeon, Y. B., Moon, S. H., Kim, O. H., Lee, D. H., & Kim, C. H. (2023). Functional characteristics of whey protein-derived peptides produced using lactic acid bacteria hydrolysis. *Journal of Dairy Science and Biotechnology, 41*(1), 34–43. https://doi.org/10.22424/jdsb.2023.41.1.34

Li, A., Zheng, N., & Ding, X. (2022). Mitochondrial abnormalities: A hub in metabolic syndrome-related cardiac dysfunction caused by oxidative stress. *Heart Failure Reviews, 27*(4), 1387–1394. https://doi.org/10.1007/s10741-021-10109-6

Lin, H., Zhao, J., Xie, Y., Tang, J., Wang, Q., Zhao, J., & Liu, P. (2024). Identification and molecular mechanisms of novel antioxidant peptides from fermented broad bean paste: A combined in silico and *in vitro* study. *Food Chemistry, 450*, Article 139297. https://doi.org/10.1016/j.foodchem.2024.139297

Lopez-Ruiz, A., Chandrashekar, K., & Juncos, L. A. (2023). Nrf2 activation in the glomeruli and podocytes: Deciphering the renal mechanisms of Nrf2. *Kidney, 4*(10), 1350–1352. https://doi.org/10.34067/KID.0000000000000268

Lu, J. J., Cheng, M. C., Khumsupan, D., Hsieh, C. C., Hsieh, C. W., & Cheng, K. C. (2023). Evaluation of fermented turmeric milk by lactic acid bacteria to prevent UV-induced oxidative stress in human fibroblast cells. *Fermentation, 9*, 230. https://doi.org/10.3390/fermentation9030230

Mahmud, S., Pitcher, L. E., Torbenson, E., Robbins, P. D., Zhang, L., & Dong, X. (2024). Developing transcriptomic signatures as a biomarker of cellular senescence. *Ageing Research Reviews.* , Article 102403. https://doi.org/10.1016/j.arr.2024.102403

Makpol, S., Durani, L. W., Chua, K. H., Mohd Yusof, Y. A., & Wan Ngah, W. Z. (2011). Tocotrienol-rich fraction prevents cell cycle arrest and elongates telomere length in senescent human diploid fibroblasts. *BioMed Research International, 1*, Article 506171. https://doi.org/10.1155/2011/506171

Marionnet, C., Pierrard, C., Lejeune, F., Sok, J., Thomas, M., & Bernerd, F. (2010). Different oxidative stress response in keratinocytes and fibroblasts of reconstructed skin exposed to non-extreme daily-ultraviolet radiation. *PLoS One, 5*, Article e12059. https://doi.org/10.1371/journal.pone.0012059

Mehboob, M. Z., & Lang, M. (2021). Structure, function, and pathology of protein O-glucosyltransferases. *Cell Death & Disease, 12*, 71. https://doi.org/10.1038/s41419-020-03314-y

Mirzaei, M., Mirdamadi, S., Ehsani, M. R., & Aminlari, M. (2018). Production of antioxidant and ACE-inhibitory peptides from *Kluyveromyces marxianus* protein hydrolysates: Purification and molecular docking. *Journal of Food and Drug Analysis, 26*, 696–705. https://doi.org/10.1016/j.jfda.2017.07.008

Moliner, C., Míguez-Mosquera, M., Llorent-Martínez, E. J., Guisantes-Batan, E., Bahrim, G. E., Fernández-de Córdova, M. L., & Ruiz-Medina, A. (2019). Viola cornuta and viola x wittrockiana: Phenolic compounds, antioxidant and neuroprotective activities on *Caenorhabditis elegans*. *Journal of Food and Drug Analysis, 27*, 849–859. https://doi.org/10.1016/j.jfda.2019.05.005

Nandita, H., Manohar, M., & Gowda, D. V. (2020). Recent review on oxidative stress, cellular senescence and age-associated diseases. *International Journal of Pharmaceutical Sciences and Research, 11*, 1331–1342. https://ijrps.com/home/article/view/806.

Odawara, T., Yamauchi, S., & Ichijo, H. (2024). Apoptosis signal-regulating kinase 1 promotes inflammation in senescence and aging. *Communications Biology, 7*(1), 691. https://doi.org/10.1038/s42003-024-06386-0

Oh, S. I., Park, J. K., & Park, S. K. (2015). Lifespan extension and increased resistance to environmental stressors by N-acetyl-L-cysteine in *Caenorhabditis elegans*. *Clinics, 70*, 380–386. https://doi.org/10.6061/clinics/2015(05)13

Olivares-Vicente, M., Sánchez-Marzo, N., Herranz-López, M., & Micol, V. (2024). Analysis of lemon verbena polyphenol metabolome and its correlation with oxidative stress under glucotoxic conditions in adipocyte. *Journal of Agricultural and Food Chemistry, 72*, 9768–9781. https://doi.org/10.1021/acs.jafc.3c06309

Ren, L. K., Yang, Y., Ma, C. M., Fan, J., Bian, X., Liu, B. X., & Zhang, N. (2022). Identification and in silico analysis of novel antioxidant peptides in broken rice protein hydrolysate and its cytoprotective effect against H2O2-induced 2BS cell model. *Food Research International, 162*, Article 112108. https://doi.org/10.1016/j.foodres.2022.112108

Rom, O., Liu, Y., Finney, A. C., Ghrayeb, A., Zhao, Y., Shukha, Y., & Chen, Y. E. (2022). Induction of glutathione biosynthesis by glycine-based treatment mitigates atherosclerosis. *Redox Biology, 52*, Article 102313. https://doi.org/10.1016/j.redox.2022.102313

Ryu, Y. S., Kang, J. I., Han, Y. K., Lim, J. M., Lee, J., & Kim, E. M. (2019). Marine compound 3-bromo-4,5-dihydroxybenzaldehyde protects skin cells against oxidative damage via the Nrf2/HO-1 pathway. *Marine Drugs, 17*, 234. https://doi.org/10.3390/md17040234

Salminen, A., Kaarniranta, K., & Kauppinen, A. (2022). Photoaging: UV radiation-induced inflammation and immunosuppression accelerate the aging process in the skin. *Inflammation Research, 71*, 817–831. https://doi.org/10.1007/s00011-022-01598-8

Sasaki, M., Kajiya, H., Ozeki, S., Okabe, K., & Ikebe, T. (2014). Reactive oxygen species promotes cellular senescence in normal human epidermal keratinocytes through epigenetic regulation of p16INK4a. *Biochemical and Biophysical Research Communications, 452*, 622–628. https://doi.org/10.1016/j.bbrc.2014.08.123

Shi, Y. C., Liao, V. H. C., & Pan, T. M. (2012). Monascin from red mold dioscorea as a novel antidiabetic and antioxidative stress agent in rats and *Caenorhabditis elegans*. *Free Radical Biology and Medicine, 52*, 109–117. https://doi.org/10.1016/j.freeradbiomed.2011.09.034

Tang, Y. C., Chang, H. H., Chen, H. H., Yao, J. Y., Chen, Y. T., Chuang, Y. J., & Kuo, C. C. (2021). A novel NRF2/ARE inhibitor gossypol induces cytotoxicity and sensitizes chemotherapy responses in chemo-refractory cancer cells. *Journal of Food and Drug Analysis, 29*, 638. https://doi.org/10.38212/2224-6614.3376

Tanigawa, S., Fujii, M., & Hou, D. X. (2007). Action of Nrf2 and Keap1 in ARE-mediated NQO1 expression by quercetin. *Free Radical Biology and Medicine, 42*, 1690–1703. https://doi.org/10.1016/j.freeradbiomed.2007.02.017

Tao, M., Li, R., Xu, T., Zhang, Z., Zheng, D., Xia, Z., & Xu, X. (2023). Vitexin and isovitexin delayed ageing and enhanced stress-resistance through the activation of the SKN-1/Nrf2 signaling pathway. *International Journal of Food Sciences & Nutrition, 74*(6), 685–694. https://doi.org/10.1080/09637486.2023.2243055

Thomas, P. D., Hill, D. P., Mi, H., Osumi-Sutherland, D., Van Auken, K., Carbon, S., & Mungall, C. J. (2019). Gene Ontology Causal Activity Modeling (GO-CAM) moves beyond GO annotations to structured descriptions of biological functions and systems. *Nature Genetics, 51*, 1429–1433. https://doi.org/10.1038/s41588-019-0500-1

Urbizo-Reyes, U., Kim, K. H., Reddivari, L., Anderson, J. M., & Liceaga, A. M. (2022). Oxidative stress protection by canary seed (*Phalaris canariensis* L.) peptides in Caco-2 Cells and *Caenorhabditis elegans. Nutrition*. https://doi.org/10.3390/nu14122415.

Vilcacundo, R., Martínez-Villaluenga, C., & Hernández-Ledesma, B. (2017). Release of dipeptidyl peptidase IV, α-amylase and α-glucosidase inhibitory peptides from quinoa (*Chenopodium quinoa* Willd.) during in vitro simulated gastrointestinal digestion. *Journal of Functional Foods, 35*, 531–539. https://doi.org/10.1016/j.jff.2017.06.024

Wang, T., Jian, Z., Baskys, A., Yang, J., Li, J., Guo, H., & Long, Q. (2020). MSC-derived exosomes protect against oxidative stress-induced skin injury via adaptive regulation of the NRF2 defense system. *Biomaterials, 257*, Article 120264. https://doi.org/10.1016/j.biomaterials.2020.120264

Wang, Z., Ma, X., Li, J., & Cui, X. (2016). Peptides from sesame cake extend healthspan of *Caenorhabditis elegans* via upregulation of skn-1 and inhibition of intracellular ROS levels. *Experimental Gerontology, 82*, 139–149. https://doi.org/10.1016/j.exger.2016.07.001

Wang, C. Y., Xu, Y., Wang, X., Wang, Y., Guo, Y., & Zhang, Z. (2016). Dl-3-n-butylphthalide-induced upregulation of antioxidant defense is involved in the enhancement of cross talk between CREB and Nrf2 in an Alzheimer's disease mouse model. *Neurobiology of Aging, 38*, 32–46. https://doi.org/10.1016/j.neurobiolaging.2015.10.024

Wu, C. W., Deonarine, A., Przybysz, A., Strange, K., & Choe, K. P. (2016). The Skp1 homologs SKR-1/2 are required for the *Caenorhabditis elegans* SKN-1 antioxidant/detoxification response independently of p38 MAPK. *PLoS Genetics, 12*(10), Article e1006361. https://doi.org/10.1371/journal.pgen.1006361

Wu, Q., Lu, F., Lei, J., Liu, Y., Zhu, N., Yu, Y., Ning, Z., & She, T. (2023). Nrf2 signaling pathway: Current status and potential therapeutic targetable role in human cancers. *Frontiers in Oncology*. https://doi.org/10.3389/fonc.2023.1184079

Xiong, L., Deng, N., Zheng, B., Li, T., & Liu, R. H. (2021). HSF-1 and SIR-2.1 linked insulin-like signaling is involved in goji berry (*Lycium* spp.) extracts promoting lifespan extension of *Caenorhabditis elegans*. *Food & Function, 12*, 7851–7866. https://doi.org/10.1039/D0FO03300F

Xu, T. H., Du, Y., Sheng, Z., Li, Y., Qiu, X., Tian, B., & Yao, L. (2022). OGT-mediated keap1 glycosylation accelerates Nrf2 degradation leading to high phosphate-induced vascular calcification in chronic kidney disease. *Frontiers in Physiology, 11*, 1092. https://doi.org/10.3389/fphys.2020.01092

Ye, Q., Li, Y., Wang, C., Zheng, J., Qiao, J., Yang, J., & Wan, Q. L. (2021). Sitagliptin extends lifespan of *Caenorhabditis elegans* by inhibiting insulin/insulin-like signaling and activating dietary restriction-like signaling pathways. *Gerontology, 70*, 90–101. https://doi.org/10.1159/000534863

Yin, B., & Jiang, X. (2013). Telomere shortening in cultured human dermal fibroblasts is associated with acute photodamage induced by UVA irradiation. *Advances in Dermatology and Allergology/Postępy Dermatologii i Alergologii, 30*, 13–18. https://doi.org/10.5114/pdia.2013.33374